Theory of gyro with rotating gimbal and flexural pivots

THEORY OF GYRO WITH ROTATING GIMBAL AND FLEXURAL PIVOTS

by

G.H.M. van Dijk

Group Measurement and Control
Department of Electrical Engineering
Eindhoven University of Technology
Eindhoven, The Netherlands

THEORY OF GYRO WITH ROTATING GIMBAL AND FLEXURAL PIVOTS

BY

G.H.M. van Dijk

T.H. Report 73-E-42

September 1972

This paper was submitted in partial fulfillment of the requirements for the degree of Ir. (M.Sc.) at the Eindhoven University of Technology. The work was carried out in the Measurement and Control Group under the directorship of Prof.dr. C.E. Mulders.
Advisor: Dipl.-Ing. C. Huber

ISBN 90 6144 042 4

Summary

The Hooke's joint is one of the several possible means for suspending a gyro free of torques. This report shows how the cross member of the Hooke's joint exerts a centrifugal torque on the gyro rotor.

A mechanical way to compensate this torque is the use of the spring torque of flexural pivots. Besides these torques a damping torque will be discussed which interferes with the ideal functioning of the suspension.

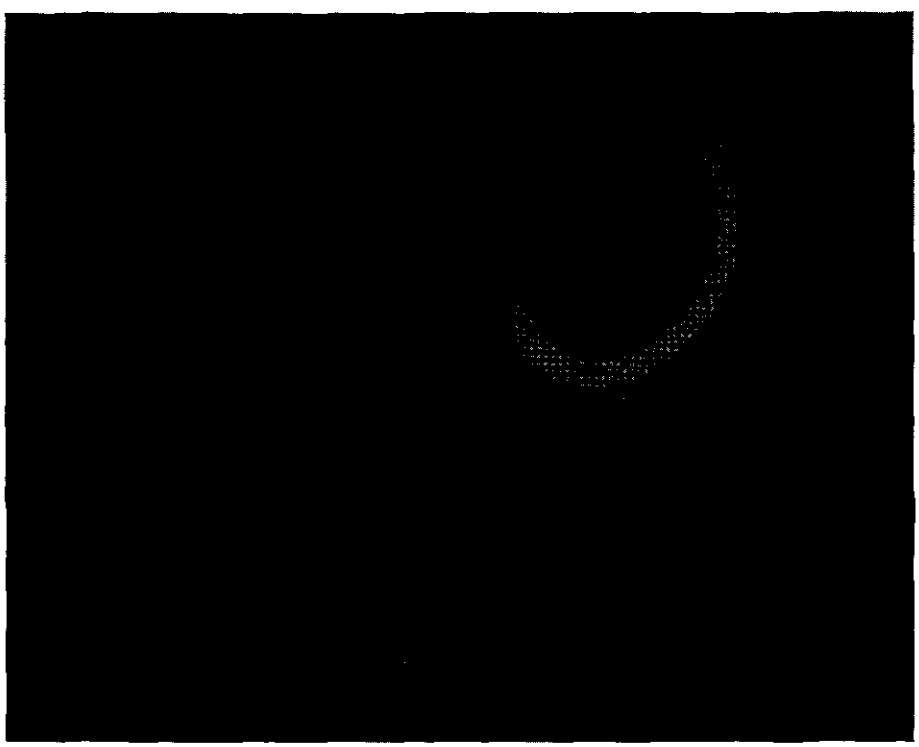

The experimental Hooke's joint gyro.

Index

1. Introduction.

1.1. Rotor suspension problems.

The gyroscope based on the principle of a spinning rotor is being widely used nowadays as inertial direction memory and as rotation sensor. The fields of application comprise stabilization, attitude control, and navigation of water, air, and space vehicles (SAVET).

Among the various design approaches the free rotor gyro, also called the two degrees of freedom gyro, is the most ancient. It is still in use to-day.

Such a free rotor gyro actually is a vector memory in inertial space, provided it is kept free of torques. By effectively suspending it in its centre of gravity torques due to gravitation and other accelerations can be well nigh eliminated. Using a Cardano gimbal system we can achieve this, at the same time isolating the gyro from rotation movements of the base or vehicle on which it is carried (MAGNUS, SAVET).

Of course any practical gimbal will have moments of inertia that can become disturbing, and the pivots necessary to realize the gimbal joints will always exhibit spurious torques however refined the execution may be. Designers have had to give this problem very much attention. They have been using ball-bearings, jewel pivots, gas bearings, magnetic bearings, flexural pivots. Each design principle has its own merits and disadvantages.

Recently, attention has increasingly been drawn to the flexural pivot suspension, as it can eliminate the need of lubrication and suspension fluids and gases. Also this type of joints makes it feasable to use internal, rotating gimbals which have certain advantages above the external, stationary gimbal systems. The flexural pivots, however, can hardly be made free of serious elastic torques, but fortunately these can be used to compensate certain mass torques.

The following treatise will examine the torques involved in the use of rotating gimbals, and the aspects of achieving torque compensation.

1.2. The aim of this article.

In the past only very few articles have appeared on the behaviour of gyros with flexural pivots suspension. They discussed experiments (ARNOLD) and they gave mathematical explanations (HOWE). We too have been experimenting with a model of this type of gyro and will give some results thereof, but the most important part of this treatise will show an explanation of the dynamical behaviour, based on the geometrical derivation of the motion of the several parts of the gyro. Some rules of vector calculation relating to perpendicular vectors are used to simplify the derivation.

It will appear that the rotating gimbal always exercises a centrifugal torque on the rotor when the spin axis of the rotor and the driving shaft axis do not coincide. In the case of flexural suspension a spring torque is available to compensate this centrifugal torque.

2. Kinematics.

In fact the rotating gimbal used is a Hooke's joint between the rotor and the driving shaft. Like an ordinary gimbal it imparts to the gyro two degrees of freedom. The whole construction consists of three parts (figure 2.-1), namely: the driving shaft (1) with a fork, which is joined by a pair of flexural pivots to the cross member (2); another pair of flexural pivots connects this member with a flywheel (3), the gyro proper.

One pair of flexural pivots is mounted between the fork and the cross member. We shall call these pivots the "fork pivots" and indicate them symbolically by their stiffness S_f. We can also draw an imaginary axis A_f through them. In the same way, between the cross member and the rotor, we find the "gyro pivots" with stiffness S_g on the axis A_g.

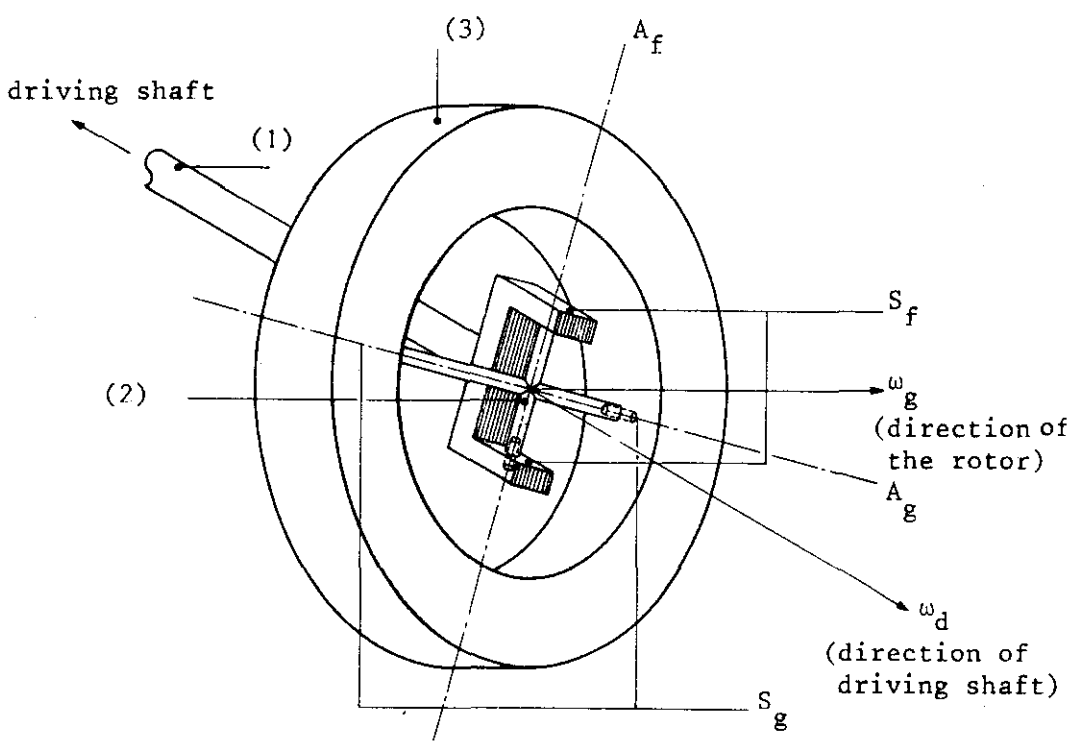

fig. 2.-1. A model of a gyro with rotating gimbal.

In the following paragraphs the axes systems will be defined, and subsequently the angular deflections, deviations, and also the velocities will be derived. With these data the movement of the cross member can finally be described.

To begin with, it is assumed that the gyro does not make a precession and so rotates in a fixed plane.

2.1. Axes systems and transformations.

Figure 2.-2 shows a highly simplified representation of the gyro. Only the axes A_f and A_g and the flexural pivots S_f and S_g are drawn. V_f and V_g are the planes in which the fork and gyro pivots, and with them the axes A_f and A_g respectively, keep rotating.

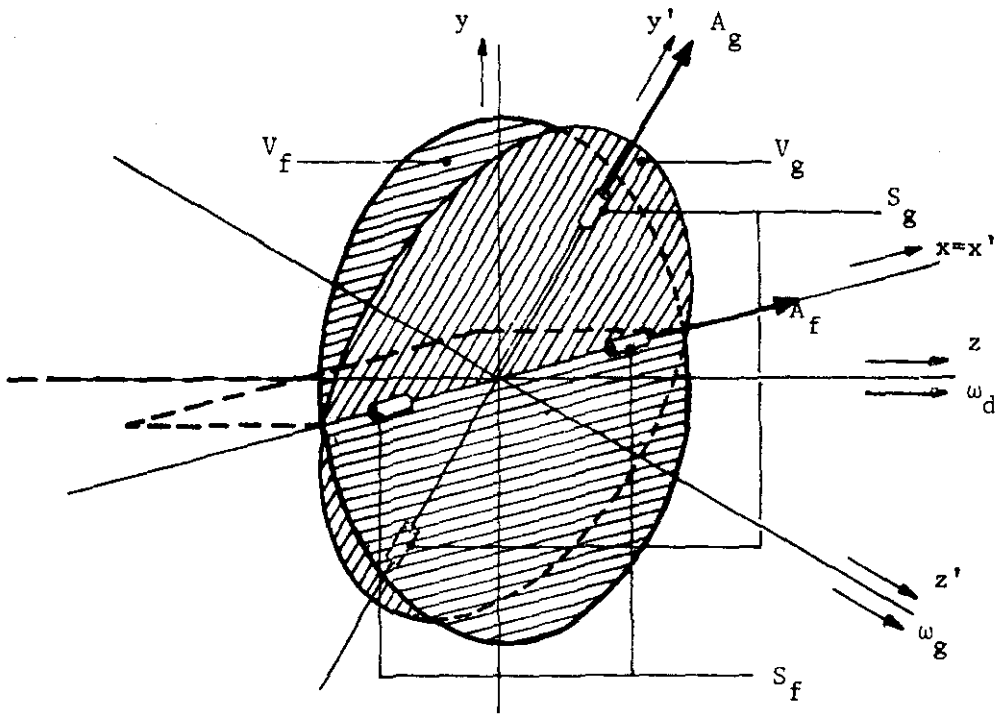

fig. 2.-2. Planes of rotation of the pivots.

The system of coordinates (x, y, z) is so chosen that the x- and y- axes are situated in the plane V_f, while the z- axis, perpendicular to this plane, coincides with the driving shaft axis. Correspondingly, the plane V_g contains the coordinates x' and y', the orientation being chosen to make the x- and the x'- axes coincide. The z'- axis represents the spin axis of the rotor. A rotation through an angle α about the x- axis transforms the one system into the other. This angle is produced by a deviation of the spin axis of the rotor

from the direction of the driving shaft axis, marked by its angular velocity ω_d. The direction of the spin axis of the rotor, the gyro proper, is indicated by the angular velocity ω_g of the gyro.
Note that both systems of coordinates remain fixed in space as the gyro is rotating. In this treatise the axes A_f and A_g will be considered to be vectors with lengths R_f and R_g. This vector notation has the advantage that the directions can be calculated simply.

The transformation of any vector $L_1(x'y'z')$ into $L_1(xyz)$ can be calculated by:

$$L_1(xyz) = \begin{pmatrix} 1 & 0 & 0 \\ 0 & \cos\alpha & -\sin\alpha \\ 0 & \alpha & \cos\alpha \end{pmatrix} \cdot L_1(x'y'z') \qquad 2.-(1)$$

Analogically any vector $L_2(xyz)$ will be transformed into $L_2(x'y'z')$ by:

$$L_2(x'y'z') = \begin{pmatrix} 1 & 0 & 0 \\ 0 & \cos\alpha & \sin\alpha \\ 0 & -\sin\alpha & \cos\alpha \end{pmatrix} \cdot L_2(xyz) \qquad 2.-(2)$$

This will be applied to the vectors A_g and A_f. The axis A_g is a time function given as a vector by: (figure 2.-(3)).

$$A_g(x'y'z') = R_g \begin{pmatrix} \cos\omega_g t_1 \\ \sin\omega_g t_1 \\ 0 \end{pmatrix} \qquad 2.-(3)$$

Using equation 2.-(1) we get

$$A_g(xyz) = R_g \begin{pmatrix} \cos\omega_g t_1 \\ \cos\alpha \cdot \sin\omega_g t_1 \\ \sin\alpha \cdot \sin\omega_g t_1 \end{pmatrix} \qquad 2.-(4)$$

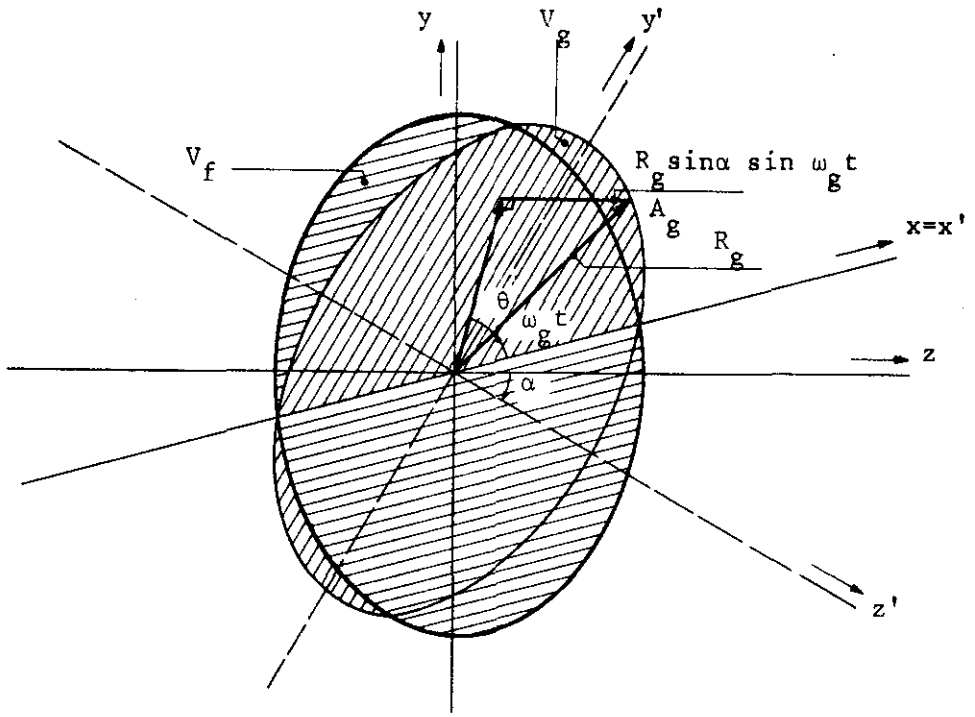

fig. 2.-3. The projection of the gyro pivot axis A_g onto the fork axis plane V_f.

The same thing can be done with A_f. From figure 2.-4 the vector A_f can be seen to be:

$$A_f(xyz) = R_f \begin{pmatrix} \cos \omega_d t_2 \\ \sin \omega_d t_2 \\ 0 \end{pmatrix} \qquad 2.-(5)$$

From equation 2.-(2) the transformation produces:

$$A_f(x'y'z') = R_f \begin{pmatrix} & \cos \omega_d t_2 \\ \cos \alpha & \sin \omega_d t_2 \\ -\sin \alpha & \sin \omega_d t_2 \end{pmatrix} \qquad 2.-(6)$$

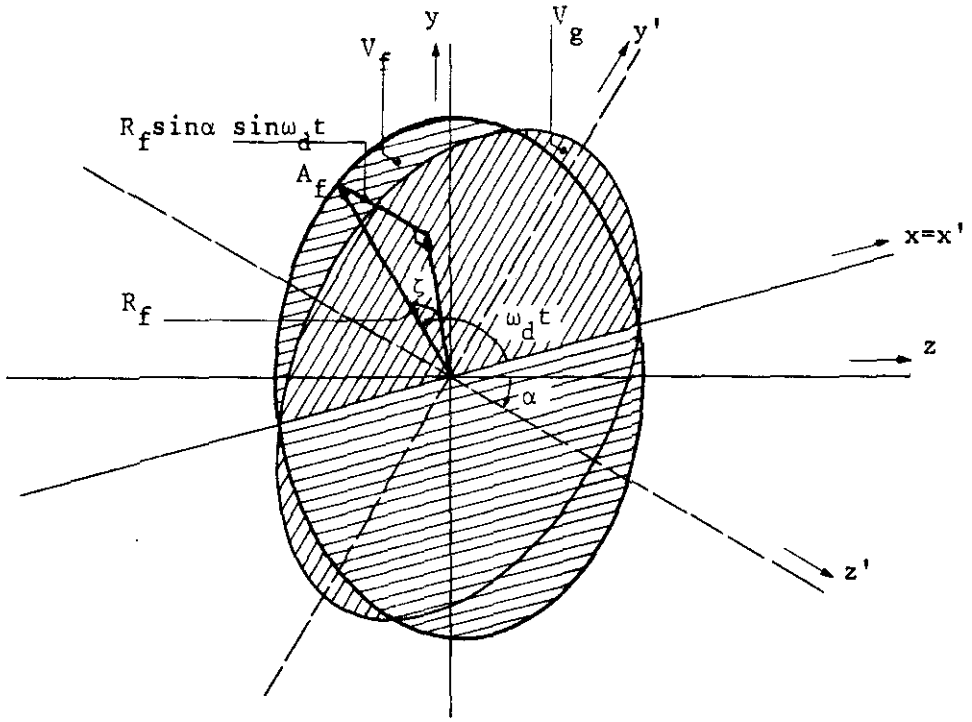

fig. 2.-4. The projection of the fork pivot axis onto the gyro plane V_g.

Up to now we assumed the gyro to be rotating in a stationary plane. In reality it will nearly always make a precession. In our case this is a rotation about the z- axis (the driving shaft axis). This means that the above mentioned systems can be completed by the transformation from the xyz- space consisting of a rotation, say θ_z, about the z- axis. This is given by the next equation.

$$L_3(x''y''z'') = \begin{pmatrix} \cos\theta_z & -\sin\theta_z & 0 \\ \sin\theta_z & \cos\theta_z & 0 \\ 0 & 0 & 1 \end{pmatrix} \cdot L_3(xyz) \qquad 2.-(7)$$

2.2. The relation between drive and precession velocities.

The axes A_f and A_g are stiffly joined perpendicular to each other. From vector calculus we know that in this case $(\underline{A}_f, \underline{A}_g) = 0$. Applying this to equations 2.-(4) and 2.-(5) we get the following results:

$$(\underline{A}_f, \underline{A}_g) = R_f.R_g(\cos \omega_g t_1 . \cos \omega_d t_2 + \cos \alpha \sin \omega_g t_1 . \sin \omega_d t_2) = 0$$

or: $\cos \omega_g t_1 . \cos \omega_d t_2 = - \cos \alpha \sin \omega_g t_1 . \sin \omega_d t_2$

From this we get:

$$\text{tang } \omega_g t_1 = \frac{- \text{cotang } \omega_d t_2}{\cos \alpha} = \frac{\text{tang}(\omega_d t_2 - \pi/2)}{\cos \alpha} \qquad 2.-(8)$$

So for $t_1 = t_2 = t$ we can conclude that the relation between $\omega_g t$ and $\omega_d t$ is:

$$\omega_g t = \text{arct}\left(\frac{\text{tang}(\omega_d t - \pi/2)}{\cos \alpha}\right) \qquad 2.-(9)$$

For the case of a small angle α this becomes

$$\omega_g t = \omega_d t - \pi/2 \qquad 2.-(10)$$

2.3. Mathematical description of the movement of the cross member.

In this part we shall concentrate our attention on the motion of the cross formed by the axes A_f and A_g because it will appear that masses outside the cross member plane defined by A_f and A_f transmit centrifugal torques to the rotor. So we are interested in the path and the velocity of such a mass. To avoid unnessecary complexity the following derivation will be given for the case of small angular displacements α only.

If we consider the line between the mass and the middle of the cross as a vector (see fig. 2.-5) then the vector product $(\underline{A}_g x \underline{A}_f)$ gives the direction of this vector.

$$\underline{A}_g(xyz) = \begin{pmatrix} \cos \omega_g t \\ \cos \alpha \cdot \sin \omega_g t \\ \sin \alpha \cdot \sin \omega_g t \end{pmatrix} \approx \begin{pmatrix} \sin \omega_d t \\ - \cos \omega_d t \\ - \alpha \cos \omega_d t \end{pmatrix} \qquad 2.-(11)$$

Note: R_g is assumed to be of unity length.

$$A_f(xyz) = \begin{pmatrix} \cos \omega_d t \\ \sin \omega_d t \\ 0 \end{pmatrix} \qquad \text{with } R_f = 1 \qquad 2.-(12)$$

The vector product of both becomes in the xyz- plane:

$$(\underline{A}_g \times \underline{A}_f) = \begin{pmatrix} \alpha \cos \omega_d t \cdot \sin \omega_d t \\ -\alpha \cos^2 \omega_d t \\ \cos^2 \omega_d t + \sin^2 \omega_d t \end{pmatrix} = \begin{pmatrix} \frac{1}{2}\alpha \sin 2\omega_d t \\ -\frac{1}{2}\alpha(\cos 2\omega_d t + 1) \\ 1 \end{pmatrix} \qquad 2.-(13)$$

We have now found analytically the path of the mass to be a circle in the plane $z = 1$ with its centre at $(0, -\alpha/2, 1)$ and a radius with length $\frac{1}{2}\alpha$. This can be expressed in:

$$\left.\begin{aligned} x^2 + (y + \tfrac{1}{2}\alpha)^2 &= \alpha^2/4 \\ z &= 1 \end{aligned}\right\} \qquad 2.-(14)$$

Equation 2.-(13) also shows, that the mass rotates along the circle with double the velocity of the driving shaft.

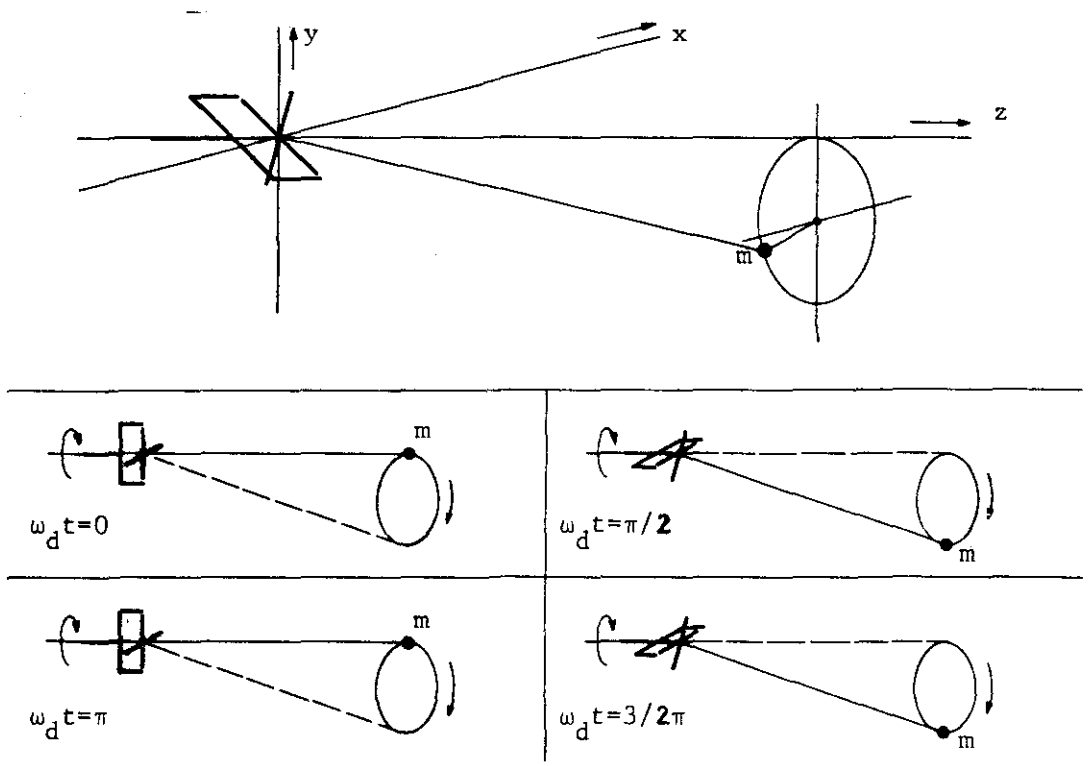

fig. 2.-5. The path of the point mass outside the plane $A_g A_f$.

The whole situation is drawn in figure 2.-4. As a matter of fact the mass does not really move in the plane z = 1, but in a plane making an angle $\alpha/2$ with this plane. This negligible fault arose from the approximation in eq. 2.-(10).

2.4. The angular displacement of the flexural pivots

The next important motion will be the momentary angular displacements of the flexural pivots, because they define the spring torques.

The displacement of S_g can be derived by determining the angle between the plane V_g and A_f (figure 2.-4). This angle, called ξ, is formed geometrically by A_f and its projection on V_g. From figure 2.-4 and equation 2.-(6) we can conclude that

$$-\xi = \arcsin\left(\frac{-R_f \sin\alpha \sin\omega_d t}{R_f}\right) \qquad 2.-(15)$$

For the case of small α this equation can be simplified into:

$$-\xi = -\alpha \sin\omega_d t \qquad 2.-(16)$$

Analogous to the above reasoning the displacement of S_f, called ζ, can be found from the angle between A_g and its projection on the plane V_f. With the help of figure 2.-3 and eq. 2.-(4) we get:

$$-\zeta = \arcsin\left(\frac{R_g \sin\alpha \sin\omega_g t}{R_g}\right) \qquad 2.-(17)$$

$\omega_g t$ is expressed as a function of $\omega_d t$ in eq. 2.-(8). Then eq. 2.-(17) becomes:

$$-\zeta = \arcsin\left(\sin\alpha \sin\left(\frac{\operatorname{arct}(\omega_d t - \pi/2)}{\cos\alpha}\right)\right) \qquad 2.-(18)$$

For small α this results in

$$-\zeta = \alpha \sin(\omega_d t - \pi/2) = -\alpha\cos\omega_d t \qquad 2.-(19)$$

3. Torques of the rotating gimbal.

There are three kinds of torques exercised upon the rotor by the rotating gimbal, i.e.: the flexural torques, a centrifugal torque and a damping torque. In this section we will discuss these torques. The first two torques will be determined with the help of the equations derived in the second chapter. The third torque has been shown by experiments and it will be formulated from these data.

3.1. The centrifugal torque.

The dynamic behaviour of an object can conveniently be examined if it is represented by an equivalent system of point masses joined perpendicular to each other with weightless rods (MAGNUS). So we shall do with the cross member. The equivalent system follows from the next figures and equations.

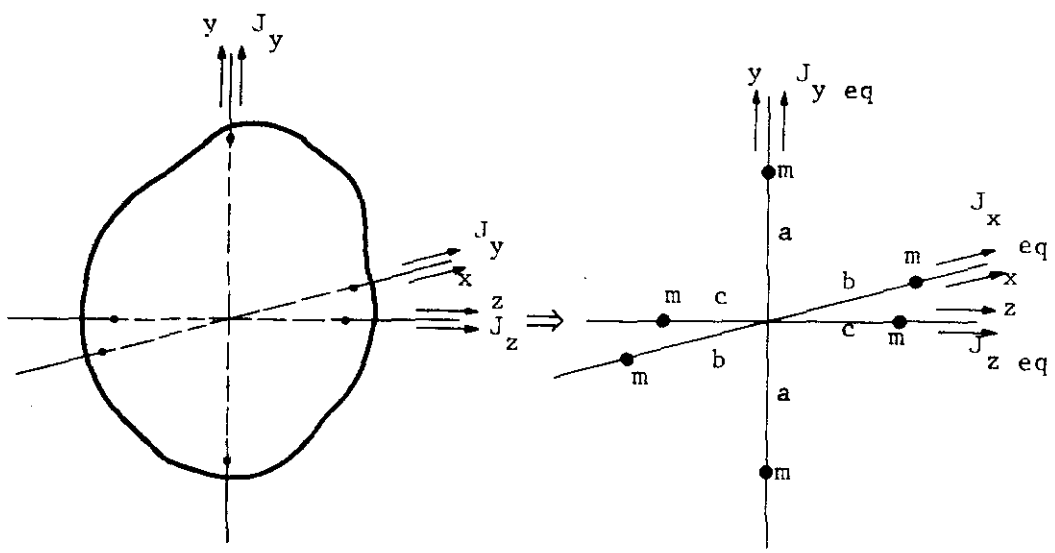

fig. 3.-1. The dynamical equivalent of anobject.

$$J_z = J_{z\ eq} = (a^2 + b^2).\ 2m$$

$$J_x = J_{x\ eq} = (a^2 + c^2).\ 2m \qquad 3.-(1)$$

$$J_y = J_{y\ eq} = (b^2 + c^2).\ 2m$$

J_x, J_y and J_z are the principal moments of inertia of the object. From this the distances a,b,c follow. For instance:

$$c^2 = \frac{J_x + J_y - J_z}{4m} \qquad 3.-(2)$$

Remark: m = 1/6 of the total mass of the object.

Applying this transformation to the cross member we get the simplified model drawn in the next figure. The positions of the masses

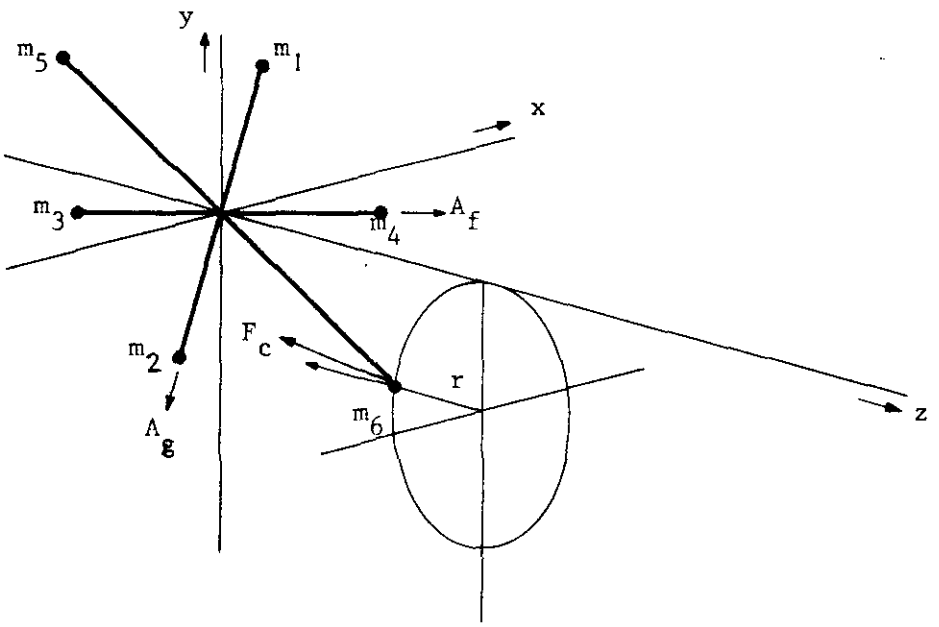

fig. 3.-2. The dynamical equivalent of the cross member.

are chosen thus, that four of them are situated on the axes A_f and A_g.

Consequently the point masses $m_{1,2}$ and $m_{3,4}$ rotate in the plane V_f and V_g respectively. It will be clear that only the masses m_5 and m_6 are able to exercise a dynamic torque. The motion of these masses is described in section 2.3. Their path is a circle which is followed with an angular velocity $2\omega_d$. Each of them senses a centrifugal force formulated by

$$F_c = m.(2\omega_d)^2.r \qquad 3.-(3)$$

The component of F_c contributing to the torque is perpendicular to the torque arm l. Since this component is $F_c . \cos \alpha$ the cosine term can be neglected for small α leaving us with F_c.

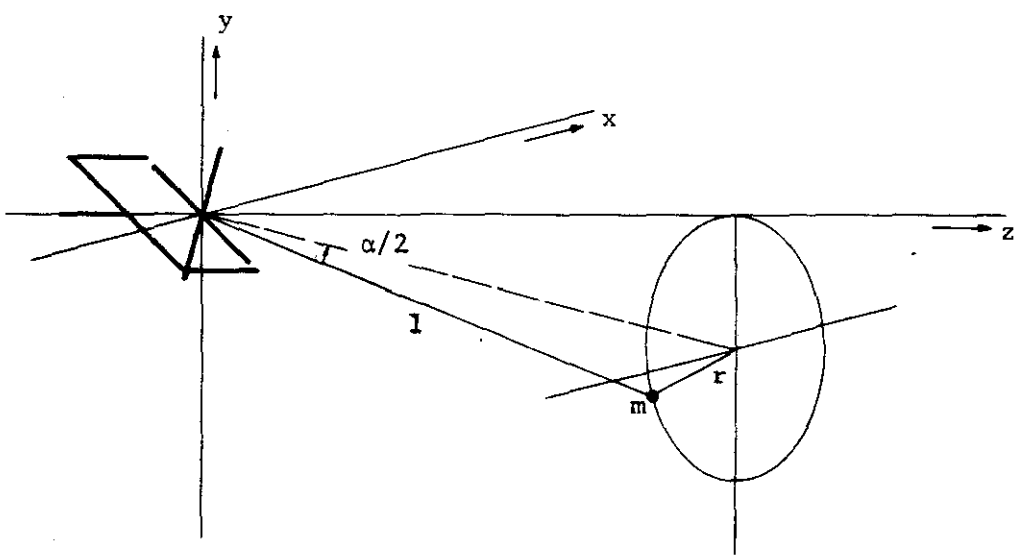

fig. 3.-3. Radius of the path of the point mass.

In the case of a small angle α we get $r = \frac{l.\alpha}{2}$ (figure 3.-3). Then eq. 3.-(3) becomes:

$$F_c = m.(2\omega_d)^2 . \frac{l.\alpha}{2} \qquad 3.-(4)$$

It is not difficult to understand that a torque sensed by the rotor must have the direction of A_f, for this is the only way to change the path of the rotor by means of a mass fixed to the cross member. This means that the torque is caused by that part of F_c perpendicular to axis A_f. Aiding to formulate this figure 3.-4 reflects the circle of a rotating mass in the plane $z = l$ and the projections of the axis A_f and the arm l on this plane. Besides that the direction of the centrifugal force F_c is also indicated.

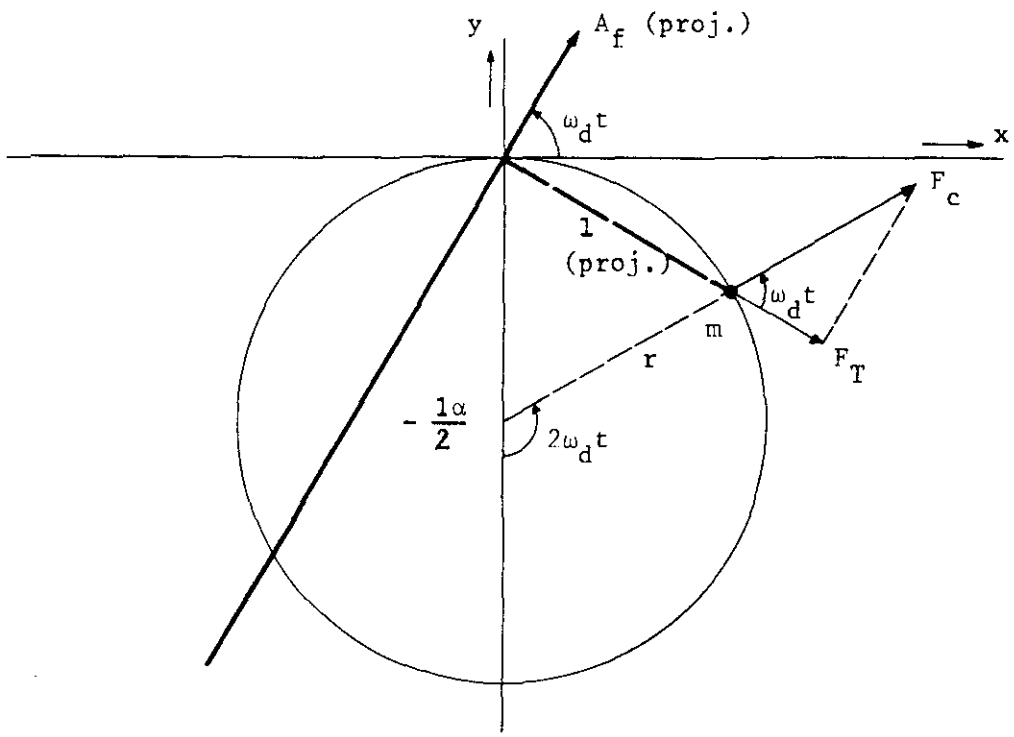

fig. 3.-4. Projection of A_f and the torque arm l. on the plane $z = l$.

We call the active component of the centrifugal force F_T. Its magnitude follows from figure 3.-4:

$$F_T = F_c \cos \omega_d t \qquad 3.-(5)$$

Then the centrifugal torque of one point mass, sensed by the rotor, will be:

$$T_{cl} = F_T . l = l . F_c \cos \omega_d t \qquad 3.-(6)$$

Using eq. 3.-(4) the torque T_{c1} becomes

$$T_{c1} = 1.m.(2\omega_d)^2 . \frac{1.\alpha}{2} . \cos \omega_d t =$$

$$= 2\ m\ \omega_d^2 . l^2 . \alpha . \cos \omega_d t \qquad 3.-(7)$$

The total centrifugal torque of both the point masses m_5 and m_6 becomes

$$\left.\begin{aligned} T_c &= 2\ T_{c1} = 4\ m\ \omega_d^2 l^2 \alpha \cos \omega_d t \\ \text{with } K &= 4\ m\ \omega_d^2 l^2 \\ T_c &= K.\alpha . \cos \omega_d t \end{aligned}\right\} \qquad 3.-(8)$$

We already had remarked above that this torque has the same direction as A_f. Then T_c as a vector follows from eq. 2.-(5)

$$T_c(xyz) = \alpha.K. \cos \omega_d t \begin{pmatrix} \cos \omega_d t \\ \sin \omega_d t \\ 0 \end{pmatrix} \qquad 3.-(9)$$

On the average over one rotation the rotor senses a torque exercised by the masses

$$T_{c\ av} = \frac{\alpha.K}{2} \begin{pmatrix} 1 \\ 0 \\ 0 \end{pmatrix} \qquad 3.-(10)$$

which is a torque acting solely in the direction of the x-axis. Looking back to eq. 3.-(2) it will be clear that: $l^2 = c^2$. Then K becomes:

$$K = 4\ m\ \omega_d^2\ l^2 = (J_c(a) + J_c(b) - J_c(c)).\ \omega_d^2 \qquad 3.-(11)$$

In this equation the parameters $J_c(a)$, $J_c(b)$ and $J_c(c)$ represent the three principal moments of inertia of the cross member.

Eqs. 3.-(9) and 3.-(10) then change to

$$T_c = \alpha.(J_c(a) + J_c(b) - J_c(c)).\ \omega_d^2.\ \cos\ \omega_d t.\ \begin{pmatrix}\cos\ \omega_d t\\ \sin\ \omega_d t\\ 0\end{pmatrix} \qquad 3.-(12)$$

Or on an average

$$\boxed{T_c = \alpha/2.(J_c(a) + J_c(b) - J_c(c)).\ \omega_d^2.\ \begin{pmatrix}1\\ 0\\ 0\end{pmatrix}} \qquad 3.-(13)$$

Should $J_c(a) + J_c(b)$ equal $J_c(c)$, then the cross member is a disk of zero thickness and the mass torque will vanish for all rotation speeds.

3.2. The flexural torques.

The flexural pivots give a torque proportional to their angular deviation. This torque is formulated by the product of the deviation and the stiffness of the pivots. Its direction is opposite to the angular displacement of the pivot. These displacements are derived in section 2.3. We can now formulate the torque $T_{v,g}$ of the flexural pivot S_g with the help of the equations 2.-(15) and 2.-(16):

$$T_{v\,g} = -\ S_g.\xi = S_g\ \arcsin(-\ \sin\ \alpha\ \sin\ \omega_d t) \qquad 3.-(14)$$

For small angles α we can simplify this equation to

$$T_{v\,g} = -\ \alpha\ S_g\ \sin\ \omega_d t \qquad 3.-(15)$$

Note: in these equations S_g represents the sum of the stiffnesses of both pivots on axis A_g.
From figure 2.-2 we can conclude, that this torque has the same direction as A_g. Then $T_{v\,g}$ as a vector becomes with equation 2.-(4):

$$T_{v\,g}(xyz) = S_g\ \arcsin(-\sin\ \alpha\ \sin\ \omega_d t)\ \begin{pmatrix}\cos\ \omega_g t\\ \cos\ \alpha\ \sin\ \omega_g t\\ \sin\ \alpha\ \sin\ \omega_g t\end{pmatrix} \qquad 3.-(16)$$

It is known from eq. 2.-(10) that $\omega_g t = \omega_d t - \pi/2$. Then eq. 3.-(16) becomes finally in the case of small angles

$$T_{v\,g}(xyz) = -\alpha\, S_g \sin\omega_d t \begin{pmatrix} \sin\omega_d t \\ -\cos\omega_d t \\ -\alpha\cos\omega_d t \end{pmatrix} \qquad 3.-(17)$$

It will be clear that the derivation of the torque $T_{v\,f}$ exercised by the pivots S_f follows an anologous way. The angular deviation ζ of S_f is expressed in eq. 2.-(18) and 2.-(19). With these equations $T_{v\,f}$ becomes

$$T_{v\,f} = -S_f.\zeta = S_f.\ \arcsin\left(\sin\alpha\,\sin\left(\frac{\operatorname{arct}(\omega_d t - \pi/2)}{\cos\alpha}\right)\right) \qquad 3.-(18)$$

For small angles α:

$$T_{v\,f} = -\,S_f\,\alpha\cos\omega_d t \qquad 3.-(19)$$

The direction of $T_{v\,f}$ is the same as $A_f(xyz)$ formulated in eq. 2.-(5). This completes the expression of $T_{v\,f}$ as a vector.

$$T_{v\,f}(xyz) = S_f.\ \arcsin\left(\sin\alpha\,\sin\left(\frac{\operatorname{arct}(\omega_d t - \pi/2)}{\cos\alpha}\right)\right)\begin{pmatrix}\cos\omega_d t\\ \sin\omega_d t\\ 0\end{pmatrix} \qquad 3.-(20)$$

Or for small α:

$$T_{v\,f}(xyz) = -\alpha\, S_f \cos\omega_d t \begin{pmatrix}\cos\omega_d t\\ \sin\omega_d t\\ 0\end{pmatrix} \qquad 3.-(21)$$

The total spring torque sensed by the rotor is formed by the vectorial sum of the torques of both pairs of pivots. This sum becomes in the case of small α

$$T_v(xyz) = T_{v\,g} + T_{v\,f} = \begin{pmatrix} -\alpha S_g \sin^2\omega_d t - \alpha S_f \cos^2\omega_d t \\ \alpha S_g \sin\omega_d t\cos\omega_d t - \alpha S_f \sin\omega_d t\cos\omega_d t \\ 0 \end{pmatrix} \qquad 3.-(22)$$

If $S_g = S_f = S$ then this expression changes into

$$T_v(xyz) = \begin{pmatrix} -\alpha S \\ 0 \\ 0 \end{pmatrix} \qquad 3.-(23)$$

If S_g and S_f are not equal then they can be formulated by

$$\begin{aligned} S_g &= S_{a\,v} - s \\ S_f &= S_{a\,v} + s \end{aligned} \qquad 3.-(24)$$

$S_{a\,v}$ is the mean value of both stiffnesses S_g and S_f. The difference from the mean value is expressed by s, which can be both positive and negative. Equation 3.-(22) now becomes

$$T_v(xyz) = \begin{pmatrix} -\alpha S_{a\,v} + \alpha\, s \sin^2 \omega_d t - \alpha\, s \cos^2 \omega_d t \\ -2\,\alpha\, s \sin \omega_d t \cos \omega_d t \\ 0 \end{pmatrix}$$

$$= \begin{pmatrix} -\alpha S_{a\,v} \\ 0 \\ 0 \end{pmatrix} - \begin{pmatrix} \alpha\, s \cos 2\,\omega_d t \\ \alpha\, s \sin 2\,\omega_d t \\ 0 \end{pmatrix} \qquad 3.-(25)$$

On the average the contribution of the latter column will be zero.
As effective torque is left

$$\boxed{T_{v\,av}(xyz) = \begin{pmatrix} -\alpha S_{a\,v} \\ 0 \\ 0 \end{pmatrix}} \qquad 3.-(26)$$

The direction of the average torque appears to be always the same whether both pivot axes have the same stiffness or not.

3.3. The damping torques.

Besides the aforementioned torques there is a damping torque. This torque has two causes. First there are the losses in the flexural pivots. Second the cross member and the rotor experience air friction. In consequence of this torque the deviation angle α will decrease. From experiments it is to be seen that this angle expires as an exponentional function of time and can be formulated by

$$\alpha = \alpha_o e^{-\rho t} \qquad 3.-(27)$$

In this equation the parameter ρ represents the damping which experiments have shown to be a function of the rotation velocity ω_d. The magnitude of the torque can be determined as follows. We shall assume that the gyro makes a precession. In figure 3.-5. the observed path of the spin axis is drawn. The dotted line is the undamped path.

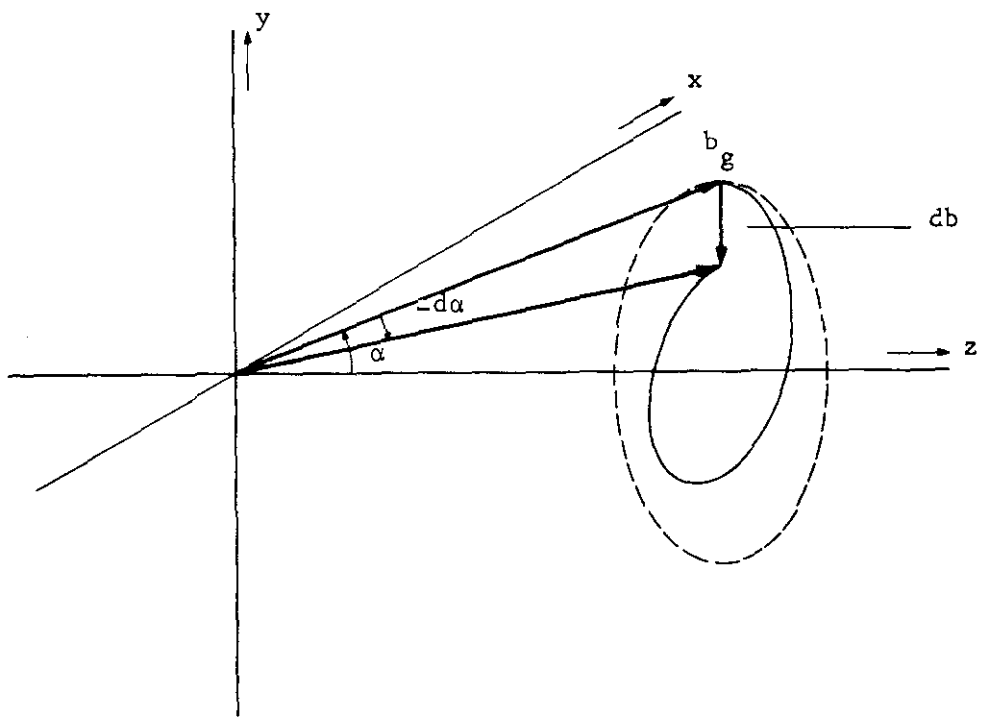

fig. 3.-5. Damped precession.

To change the direction of the spin axis a torque perpendicular to it is always necessary. From the way the gyro drifts it is clear that this damping torque points towards the driving shaft. The figure shows that

$$db = - b_g \, d\alpha$$ (where $b_g = J_g(c)$. ω_g = angular momentum of the rotor)

From literature about gyros it is well known that a torque changing the direction of the spin axis can be formulated as

$$T = \frac{db}{dt}$$

With the help of eq. 3.-(27) the damping torque can now be formulated

$$T_{damp} = - b_g \frac{d\alpha}{dt} = -b_g . -\rho . \alpha_o e^{-\rho t} = b_g . \rho . \alpha . = \alpha . J_g . \omega_g . \rho \qquad 3.-(28)$$

It is not easy to reason the origin, the momentary direction and magnitude of this torque. Therefore the parameter ρ can most conveniently be determinated with the help of experiments.

4. Gyro responses to gimbal torques.

4.1. Responses to the centrifugal and the flexural torques.

From the sections above it appears that the flexural pivots and the cross member exercise torques on the rotor. These have the character of positive and negative spring torques. As long as they do not compensate each other they cause a precession of the rotor. During this motion the resulting average torque is always perpendicular to b_g and ω_d. Geometrically we can find the precession velocity with the help of the figure 4.-1.

The precession can be calculated from T and the component of b_g which is perpendicular to the driving shaft. The precession velocity then

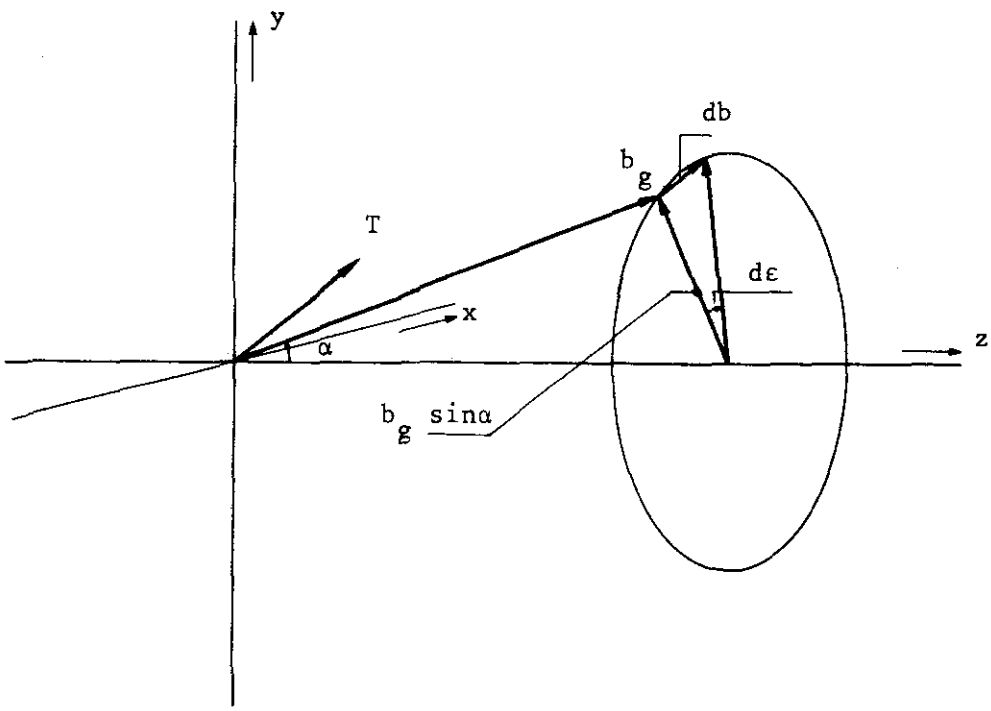

fig. 4.-1. Precession cone.

follows from

$$\omega_p = \frac{d\varepsilon}{dt} \qquad 4.-(1)$$

To change the direction of b_g we have to add to b_g

$$db = b_g (\sin \alpha) \cdot d\varepsilon .$$

This requires a torque $T = \frac{db}{dt}$.
From the combination of both we get

$$b_g (\sin \alpha) d\varepsilon = T\, dt \qquad 4.-(2)$$

With equation 4.-(1) the precession velocity ω_p becomes

$$\omega_p = \frac{T}{b_g \sin \alpha} \qquad 4.-(3)$$

For small α:

$$\omega_p = \frac{T}{b_g \cdot \alpha} \qquad 4.-(4)$$

The torque T is the sum of the centrifugal and the flexural torques. Their average values are expressed in the eqs. 3.-(10) and 3.-(23). The magnitude of the total torque in the direction drawn in figure 4.-1 becomes

$$T = \frac{\alpha K}{2} - \alpha S \qquad 4.-(5)$$

With $K = 4\, m\, \omega_d^2\, l^2$ or $K = (J_c(a) + J_c(b) - J_c(c))\omega_d^2$

Substitute eq. 4.-(5) into eq. 4.-(4) to receive

$$\omega_p = \frac{\alpha(\frac{1}{2}K - S)}{b_g \cdot \alpha} = \frac{\frac{1}{2}K - S}{b_g} \qquad 4.-(6)$$

$$\omega_p = \frac{1}{J_g(c)}\left(\tfrac{1}{2}\omega_d (J_c(a) + J_c(b) - J_c(c)) - \frac{S}{\omega_d}\right) =$$

$$= \frac{1}{J_g(c)}\left(M\omega_d - \frac{S}{\omega_d}\right) \quad \text{with } M = \tfrac{1}{2}(J_c(a) + J_c(b) - J_c(c)) \qquad 4.-(7)$$

Should $M\,\omega_d$ be greater than $\frac{S}{\omega_d}$ then the rotating direction of the precession is positive, otherwise negative. The precession velocity is independant of the angular deviation α.

4.2. Other oscillations.

If we are interested in the other oscillations, then the geometrical method becomes intricate. So we have to describe the equations of motion of the gyro with respect to an inertially stationary system. As the latter the coordinates x"y"z" are so chosen, that the z" axis coincides with the driving shaft axis. All of the coordinates are fixed in the intertial space. So also the driving shaft axis. We shall assume that there are no external torques and that the spin axis has got a small angular displacement from an earlier cause. The transformation of any vector L_3 of the xyz-space into the x"y"z"-space is already given in equation 2.-(7):

$$L_3(x"y"z") = \begin{pmatrix} \cos\theta_{z"} & -\sin\theta_{z"} & 0 \\ \sin\theta_{z"} & \cos\theta_{z"} & 0 \\ 0 & 0 & 0 \end{pmatrix} \cdot L_3(xyz) \qquad 4.-(8)$$

Note: $\theta_{z"}$ means the angular deflection about the z"-axis, which coincides with the z-axis.

The required motion can be approximated by the following two differential equations. They are described in many books about gyros. Therefore we shall use them without discussion.

$$\left.\begin{aligned} T_{x"} - J_{x"}\,\frac{d^2\theta_{x"}}{dt^2} - D_{x"}\,\frac{d\theta_{x"}}{dt} &= b_g\,\frac{d\theta_{y"}}{dt} \\ T_{y"} - J_{y"}\,\frac{d^2\theta_{y"}}{dt^2} - D_{y"}\,\frac{d\theta_{y"}}{dt} &= -\,b_g\,\frac{d\theta_{x"}}{dt} \end{aligned}\right\} \qquad 4.-(9)$$

$\theta_{x"}$ and $\theta_{y"}$ are rotations about the respective axes. $J_{x"}$ and $J_{y"}$ are the principle moments of inertia of the rotor. $D_{x"}$ and $D_{y"}$ are damping parameters. $T_{x"}$ and $T_{y"}$ are the components of the centrifugal and the flexural torques in the direction of x" and y".

Calculating both torques $T_{x''}$ and $T_{y''}$ the average torques of $T_v(xyz)$ and $T_c(xyz)$ have to be transformed from the xyz-system into the x"y"z"-system. After vectorially summing the flexural 3.-(25) and the centrifugual 3.-(9) torques we have

$$T(xyz) = T_v(xyz) + T_c(xyz) = -\alpha \begin{pmatrix} S_a\, v \\ 0 \\ 0 \end{pmatrix} + \alpha \begin{pmatrix} \frac{1}{2}K \\ 0 \\ 0 \end{pmatrix} =$$

$$= \alpha \begin{pmatrix} \frac{1}{2}K - S_a\, v \\ 0 \\ 0 \end{pmatrix} = \alpha \begin{pmatrix} A \\ 0 \\ 0 \end{pmatrix} \qquad 4.-(10)$$

Then transforming this with the help of equation 4.-(2) we get

$$T(x"y"z") = \alpha \begin{pmatrix} A \cos \theta_{z"} \\ A \sin \theta_{z"} \\ 0 \end{pmatrix} \qquad 4.-(11)$$

To recognize $\theta_{x"}$, $\theta_{y"}$ and $\theta_{z"}$ we have to express the angle deviation α as a vector. From the choice of the xyz system, in section 2, it is clear that $\alpha(xyz)$ will be

$$\alpha(xyz) = \alpha \begin{pmatrix} 1 \\ 0 \\ 0 \end{pmatrix}$$

Transformed into the x"y"z"-system we get the components of the deviation α about the x"-, y"- and z"-axes.

$$\alpha(x"y"z") = \alpha \begin{pmatrix} \cos \theta_{z"} \\ \sin \theta_{z"} \\ 0 \end{pmatrix} = \begin{pmatrix} \theta_{x"} \\ \theta_{y"} \\ \theta_{z"} \end{pmatrix} \qquad 4.-(12)$$

Then eq. 4.-(11) changes into

$$T(x"y"z") = \begin{pmatrix} A\, \theta_{x"} \\ A\, \theta_{y"} \\ 0 \end{pmatrix} \qquad 4.-(13)$$

Note: we shall use in the further part of this section a simplified notation:

$x'' \Rightarrow 1$

$y'' \Rightarrow 2$

Substituting eq. 4.-(13) in 4.-(9) and neglecting D_1 and D_2 we get

$$\left.\begin{aligned} A\,\theta_1 - J_1 \frac{d^2\theta_1}{dt^2} &= b_g \frac{d\theta_2}{dt} \\ A\,\theta_2 - J_2 \frac{d^2\theta_2}{dt^2} &= -\,b_g \frac{d\theta_1}{dt} \end{aligned}\right\} \qquad 4.-(14)$$

With Laplace transformation:

$$\mathcal{L}\{\theta_1\} = \theta_1(p)$$

$$\mathcal{L}\{\theta_2\} = \theta_2(p)$$

The equations change into:

$$\left.\begin{aligned} (A - J_1 p^2)\theta_1(p) &= b_g p.\theta_2(p) \\ (A - J_2 p^2)\theta_2(p) &= -b_g p.\theta_1(p) \end{aligned}\right\} \qquad 4.-(15)$$

The solution of the equations gives

$$-(b_g p)^2 = (A - J_1 p^2).(A - J_2 p^2) \qquad 4.-(16)$$

In our case of a symmetrical gyro $J_1 = J_2 = J$. This changes the expression into

$$J^2 p^4 + (b_g^2 - 2\,JA)p^2 + A^2 = 0 \qquad 4.-(17)$$

Replacing p^2 by a the equation becomes

$$J^2a^2 + (b_g^2 - 2\,JA)\,a + A^2 = 0 \qquad 4.-(18)$$

$$a_{1,2} = \frac{-(b_g^2 - 2\,JA) \pm \sqrt{b_g^4 - 4\,JA\,b_g^2}}{2\,J^2} =$$

$$= \frac{-b_g^2\left(1 - \frac{2\,AJ}{b_g^2}\right) \pm \sqrt{b_g^4\left(1 - \frac{4\,AJ}{b_g^2}\right)}}{2\,J^2} \qquad 4.-(19)$$

Replacing $\frac{2\,AJ}{b_g^2}$ by γ simplifies this equation into

$$a_{1,2} = \frac{A}{J.\gamma}\left\{(\gamma - 1) \pm \sqrt{(1 - 2\gamma)}\right\} \qquad 4.-(20)$$

The magnitude of γ easily becomes lower than unity. For our experimental gyro this point was achieved at a velocity of 120 rpm.
We can thus approximate equation 4.-(20) by

$$a_{1,2} = \frac{A}{J\gamma}\left((\gamma - 1) \pm (1 - \gamma - \tfrac{1}{2}\gamma^2 \ldots)\right) \qquad 4.-(21)$$

If we neglect all the terms of higher order than two, then the first oscillation frequency follows from:

$$p_{1,2} = \pm\sqrt{a_1} = \pm\, j\sqrt{\frac{A\gamma}{2\,J}} = \pm\frac{A}{b_g} = \pm\, j\,\frac{(\tfrac{1}{2}K - S_a\,v)}{b_g} \qquad 4.-(22)$$

This expression is again the precession frequency, that we also found in section 4.1.

The second mode of oscillation follows from the next calculation.

$$a_2 = \frac{A}{2\,J\gamma}\,(\gamma^2 + 4\,\gamma - 4) \approx \frac{A}{2\,J\gamma}(4\,\gamma - 4)$$

$$= \frac{b_g^2}{J^2}(\gamma - 1) \qquad 4.-(23)$$

$$p_{3,4} = \pm\, j\frac{b_g}{J}\sqrt{(1 - \gamma)} \approx \pm\, j\,\frac{b_g}{J}(1 - \tfrac{1}{2}\gamma) =$$

$$= \pm\, j\frac{b_g}{J}\left(1 - \frac{AJ}{b_g^2}\right) \qquad 4.-(24)$$

This is the nutational frequency of the gyro. If the torques, flexural and centrifugal, compensate each other then this becomes

$$\omega_n = \frac{b_g}{J} = \frac{J_g\omega_d}{J} \qquad 4.-(25)$$

This is the nutational frequency of the technical free gyro, well known from the literature (MAGNUS).

4.3. Compensation of the torques.

We had already remarked, that the torques exercised by the flexural pivots and the cross member can be considered as resp. a positive and a negative spring torque. So on becoming equal they are able to compensate each other. In eqs. 3.-(13) and 3.-(26) both torques are expressed as the average over one rotation of the rotor. After summing them we get

$$T_{tot} = \begin{pmatrix} \frac{1}{2}\alpha K \\ 0 \\ 0 \end{pmatrix} + \begin{pmatrix} -\alpha\, S_{a\,v} \\ 0 \\ 0 \end{pmatrix} \qquad 4.-(26)$$

This torque becomes zero if:

$$S_{a\,v} = \tfrac{1}{2}K = \tfrac{1}{2}\omega_d^2(J_c(a) + J_c(b) - J_c(c)) \qquad 4.-(27)$$

Looking back to eq. 4.-(6) it appears that at this point the precession velocity decreases to zero.

$$\omega_p = \frac{\frac{1}{2}K - S}{b_g} = 0$$

We have now formulated the condition of compensation of the average torques. More accurate will be to compensate the torques at every moment. The momentary values of the torques are expressed in eq. 3.-(12) and 3.-(25). The total torque becomes

$$T_{tot}(xyz) = \alpha K \underbrace{\begin{pmatrix} \cos^2 \omega_d t \\ \cos\ \omega_d t\ \sin\ \omega_d t \\ 0 \end{pmatrix}}_{T_c(xyz)} + \underbrace{\begin{pmatrix} -\alpha S_{a\ v} \\ 0 \\ 0 \end{pmatrix} - \begin{pmatrix} \alpha s \cos\ 2\ \omega_d t \\ \alpha s \sin\ 2\ \omega_d t \\ 0 \end{pmatrix}}_{T_v(xyz)} =$$

$$= \alpha \begin{pmatrix} \frac{1}{2}K \cos\ 2\ \omega_d t - s \cos\ 2\ \omega_d t \\ \frac{1}{2}K \sin\ 2\ \omega_d t - s \sin\ 2\ \omega_d t \\ 0 \end{pmatrix} + \alpha \begin{pmatrix} \frac{1}{2}K - S_{a\ v} \\ 0 \\ 0 \end{pmatrix} \qquad 4.-(28)$$

From the condition making the torque zero at every moment we get

$$\left.\begin{aligned} \tfrac{1}{2}K - S_{a\ v} &= 0 \\ \tfrac{1}{2}K - s &= 0 \end{aligned}\right\} \qquad 4.-(29)$$

In fact this means

$$\left.\begin{aligned} S_g &= S_{a\ v} - s = \tfrac{1}{2}K - \tfrac{1}{2}K = 0 \\ S_f &= S_{a\ v} + s = \tfrac{1}{2}K + \tfrac{1}{2}K = K \end{aligned}\right\} \qquad 4.-(30)$$

So we conclude that the ideal tuning has to obey two conditions. First the stiffness of the flexural pivots joining the gyro with the cross member have to be zero. Second the spring torque of the other has to equal the double of the average centrifugal torque.

Now there still remains the damping torque discussed in section 3.-(3) The only way to compensate this torque will be by exercising an external torque on the rotor, for instance electro-magnetically.

5. Experiments

The experimental model of the gyro which was used by us was designed and built by instrument makers of the Technological University of Eindhoven. The picture on the front page shows this instrument. It is clearly to be seen that the whole construction consists of three parts: 1) The fork; 2) the cross member , or rotating gimbal, and 3) the rotor, the gyro proper.

The motion of the gyro is detected using the approximation detector PR 9373 (Philips made). This instrument measures the distance changes between itself and a metal object. Because we had six trigger marks on the rotor, we were also able to detect the angular velocity of the gyro by means of this instrument.

The distance between the front of the rotor and the detector is plotted in figure 5.-1. as a function of time. The rotor velocity was 4000 rpm.. The decreasing of the displacement is easily to be seen and appears to be an exponentional function of time. From this the parameter ρ can be determined. The number of oscillations per unit of time forms the precession velocity. A series of these plots gives the relation between the angular velocity of the gyro and the precesion velocity. Figure 5.-2. shows the result of this experiment. At the velocity of about 5800 rpm the two torques compensate each other and the precession becomes zero. At this point the gyro will be "free". Before this point the spin axis precesses to the right, beyond this point to the left.

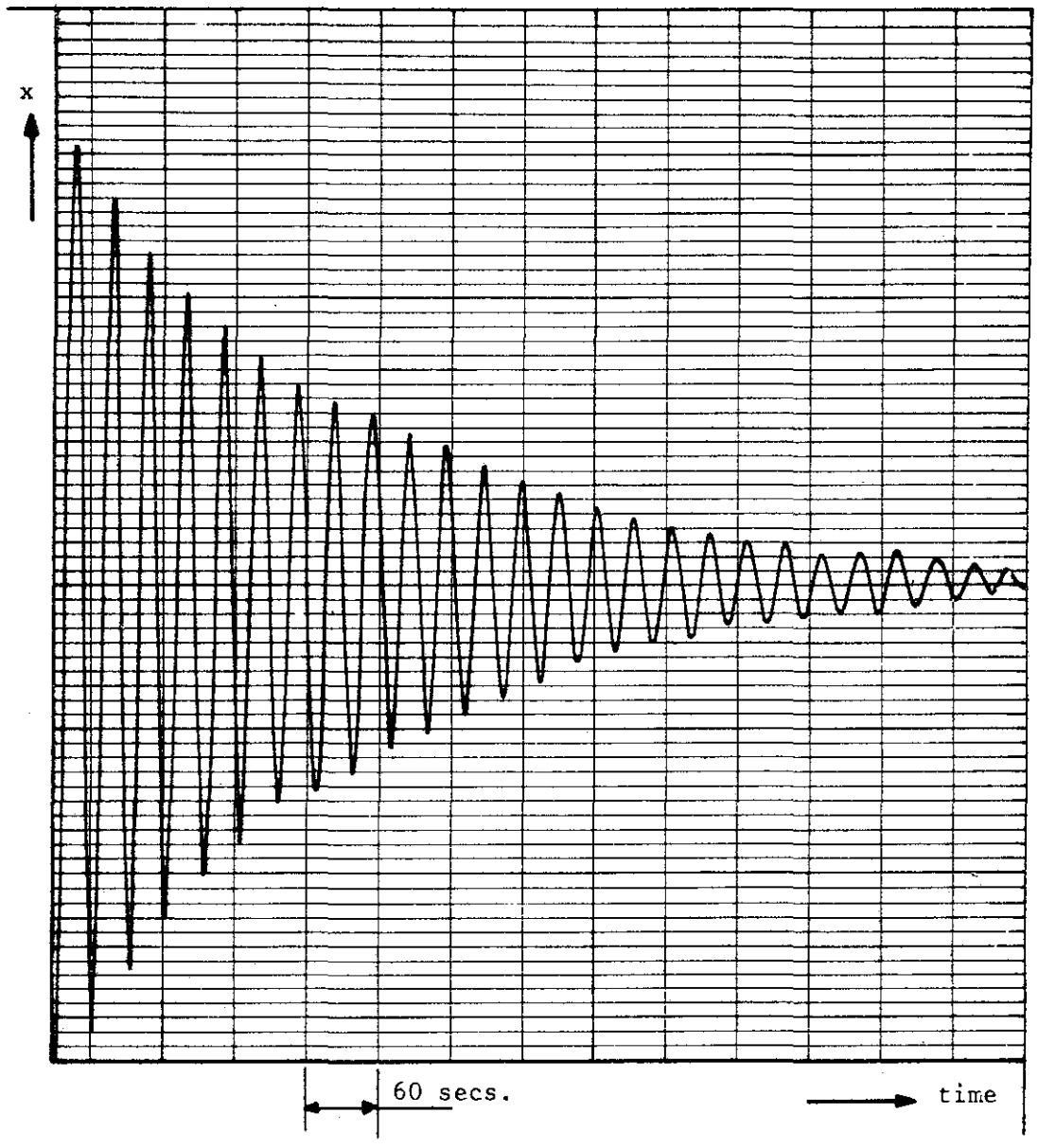

Fig. 5.-1. The distance between the front of the rotor and the sensor as a function of time. This figure shows the precession and the damping of this precession.
The angular velocity of the gyro was 4000 rpm. (paper velocity: 600 mm/h).

(precession velocity)

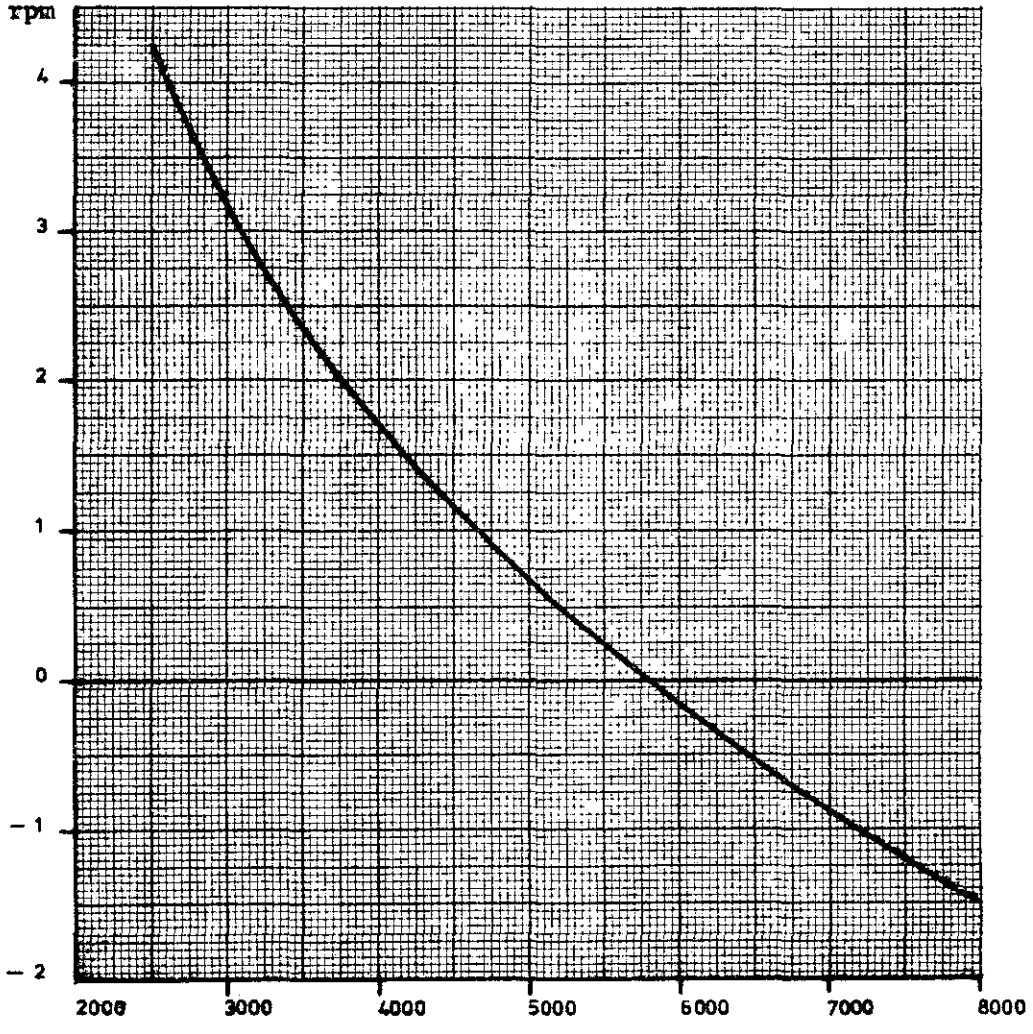

Fig. 5.-2. The relation between the angular velocity of the rotor and the precession velocity.

6. Conclusion.

This treatise has shown that the cross member of the Hooke's joint nearly always exercises a centrifugal torque on the rotor. Making use of the torque of flexural pivots this can be compensated. From experiments it appears that this theory is right. It is possible to realize a free gyro in this way.

The practical execution of course poses several problems. Two of these are:

1. The flexural pivots allow the gyro only a small angular deviation. Therefore a construction is necessary to correct the direction of the driving shaft quickly and precisely.
2. In the practical realization always an external torque is necessary to compensate the damping torques discussed in section 3.3.

7. References.

Arnold R.N.; The motion due to slow precession of gyroscope driven and supported by a Hooke's joint. Proc. Instn. mech. Engrs. London 1952, (Series B) 1B, No 3, 77.

Howe, E.W. and Savet P.H.; The dynamically tuned free rotor gyro. Control Engineering, Vol. 11, No. 6, June 1964, p. 67-72.

Magnus, K.; Kreisel, Theorie und Anwendungen. Springer Verlag, Berlin 1971

Savet, P.H.; Gyroscopes: Theory and Design. McGraw-Hill, New York, 196.

Symbols.

A_f	the fork pivot axis
A_g	gyro pivot axis
R_f	fork pivot axis vector
R_g	gyro pivot axis vector
S_f	the stiffness of the pair of flexural pivots on axis A_f
S_g	the stiffness of the pair of flexural pivots on axis A_g
α	angular deviation of the rotor
ω_d	angular velocity of the driving shaft
ω_g	angular velocity of the gyro
ω_p	precession velocity
ξ	momentary angular displacement of the flexural pivots S_g
ζ	momentary angular displacement of the flexural pivots S_f
F_c	centrifugal force
T_c	centrifugal torque sensed by the rotor
$T_{v\,g}$	flexural torque exercised by the flexural pivots S_g
$T_{V\,f}$	flexural torque exercised by the flexural pivots S_f
T_v	the vectorial sum of both torques $T_{v\,g}$ and $T_{v\,f}$+
T_d	the damping torque
$J_g(a)$, $J_g(b)$, $J_g(c)$	principal moments of inertia of the rotor
$J_c(a)$, $J_c(b)$, $J_c(c)$	principal moments of inertia of the cross member
b_g	angular momentum of the rotor
V_f	plane in which the pivots S_f rotate
x,y.z	coordinate system in the V_f plane
x',y',z'	coordinate system in the V_g plane
x",y",z"	inertial system of coordinates

EINDHOVEN UNIVERSITY OF TECHNOLOGY

THE NETHERLANDS

DEPARTMENT OF ELECTRICAL ENGINEERING

TH-Reports:

1. Dijk, J., M. Jeuken and E.J. Maanders
   AN ANTENNA FOR A SATELLITE COMMUNICATION GROUND STATION (PROVISIONAL ELECTRICAL DESIGN). TH-report 60-E-01. March 1968. ISBN 90 6144 001 7.
2. Veefkind, A., J.H. Blom and L.H.Th. Rietjens.
   THEORETICAL AND EXPERIMENTAL INVESTIGATION OF A NON-EQUILIBRIUM PLASMA IN A MHD CHANNEL. TH-report 68-E-2. March 1968. ISBN 90 6144 002 5.
   Submitted to the Symposium on a Magnetohydrodynamic Electrical Power Generation, Warsaw, Poland, 24-30 July, 1968.
3. Boom, A.J.W. van den and J.H.A.M. Melis.
   A COMPARISON OF SOME PROCESS PARAMETER ESTIMATING SCHEMES.
   TH-report 68-E-03. September 1968. ISBN 90 6144 003 3.
4. Eykhoff, P., P.J.M. Ophey, J. Severs and J.O.M. Oome.
   AN ELECTROLYTIC TANK FOR INSTRUCTIONAL PURPOSES REPRESENTING THE COMPLEX-FREQUENCY PLANE. TH-report 68-E-04. September 1968. ISBN 90 6144 004 1.
5. Vermij, L. and J.E. Daalder.
   ENERGY BALANCE OF FUSING SILVER WIRES SURROUNDED BY AIR.
   TH-report 68-E-05. November 1968. ISBN 90 6144 005 X.
6. Houben, J.W.M.A. and P. Massee.
   MHD POWER CONVERSION EMPLOYING LIQUID METALS.
   Th-Report 69-E-06. February 1969. ISBN 90 6144 006 8.
7. Heuvel, W.M.C. van den and W.F.J. Kersten.
   VOLTAGE MEASUREMENT IN CURRENT ZERO INVESTIGATIONS.
   Th-Report 69-E-07. September 1969. ISBN 90 6144 007 6.
8. Vermij, L.
   SELECTED BIBLIOGRAPHY OF FUSES.
   TH-Report 69-E-08. September 1969. ISBN 90 6144 008 4.
9. Westenberg, J.Z.
   SOME IDENTIFICATION SCHEMES FOR NON-LINEAR NOISY PROCESSES.
   TH-Report 69-E-09. December 1969. ISBN 90 6144 009 2.
10. Koop, H.E.M., J. Dijk and E.J. Maanders.
    ON CONICAL HORN ANTENNAS.
    TH-Report 70-E-10, February 1970. ISBN 90 6144 010 6.
11. Veefkind, A.
    NON-EQUILIBRIUM PHENOMENA IN A DISC-SHAPED MAGNETOHYDRODYNAMIC GENERATOR.
    TH-Report 70-E-11. March 1970. ISBN 90 6144 011 4.
12. Jansen, J.K.M., M.E.J. Jeuken and C.W. Lambrechtse.
    THE SCALAR FEED.
    TH-Report 70-E-12. December 1969. ISBN 90 6144 012 2
13. Teuling, D.J.A.
    ELECTRONIC IMAGE MOTION COMPENSATION IN A PORTABLE TELEVISION CAMERA.
    TH-Report 70-E-13. 1970. ISBN 90 6144 013 0.
14. Lorencin, M.
    AUTOMATIC METEOR REFLECTIONS RECORDING EQUIPMENT.
    TH-Report 70-E-14. November 1970. ISBN 90 6144 014 9.
15. Smets, A.J.
    THE INSTRUMENTAL VARIABLE METHOD AND RELATED IDENTIFICATION SCHEMES.
    TH-Report 70-E-15. November 1970. ISBN 90 6144 015 7.
16. White, Jr., R.C.
    A SURVEY OF RANDOM METHODS FOR PARAMETER OPTIMIZATION.
    TH-Report 70-E-16. February 1971. ISBN 90 6144 [illegible] 5.
17. Talmon, J.L.
    APPROXIMATED GAUSS-MARKOV ESTIMATORS AND RELATED SCHEMES.
    TH-Report 71-E-17. February 1971. ISBN 90 6144 017 3.
18. Kaláśek, V.
    MEASUREMENT OF TIME CONSTANTS ON CASCADE D.C. ARC IN NITROGEN.
    TH-Report 71-E-18. February 1971. ISBN 90 6144 018 1.
19. Bosselet, L.M.L.H.
    OZONBILDUNG MITTELS ELEKTRISCHER ENTLADUNGEN.
    TH-Report 71-E-19. March 1971. ISBN 90 6144 019 X.
20. Arts, M.G.J.
    ON THE INSTANTANEOUS MEASUREMENT OF BLOODFLOW BY ULTRASONIC MEANS.
    TH-Report 71-E-20. May 1971. ISBN 90 6144 020 3.
21. Koer, Th. G. van de
    NON-ISO THERMAL ANALYSIS OF CARRIER WAVES IN A SEMICONDUCTOR.
    TH-Report 71-E-21. August 1971. ISBN 90 6144 021 1.
22. Jenken, P.J., C. Huber and C.E. Mulders.
    SENSING INEPTIAL ROTATION WITH TUNING FORKS.
    TH-Report 71-E-22. September 1971. ISBN 90 6144 022 X.

23. Dijk, J. and E.J. Maanders
APERTURE BLOCKING IN CASSEGRAIN ANTENNA SYSTEMS. A REVIEW.
TH-Report 71-E-23. September 1971. ISBN 90 6144 023 8

24. Kregting, J. and R.C. White, Jr.
ADAPTIVE RANDOM SEARCH.
TH-Report 71-E-24. October 1971. ISBN 90 6144 024 6

25. Damen, A.A.H. and H.A.L. Piceni.
THE MULTIPLE DIPOLE MODEL OF THE VENTRICULAR DEPOLARISATION
TH-Report 71-E-25. October 1971. ISBN 90 6144 025 4

26. Bremmer, H.
A MATHEMATICAL THEORY CONNECTING SCATTERING AND DIFFRACTION PHENOMENA INCLUDING BRAGG-TYPE INTERFERENCES.
TH-Report 71-E-26. December 1971. ISBN 90 6144 026 2.

27. Bokhoven, W.M.G. van
METHODS AND ASPECTS OF ACTIVE-RC FILTERS SYNTHESIS.
TH-Report 71-E-27. 10 December 1970. ISBN 90 6144 027 0.

28. Boeschoten, F.
TWO FLUIDS MODEL REEXAMINED.
TH-Report 72-E-28. March 1972. ISBN 90 6144 028 9.

29. Rietjens, L.H.Th.
REPORT ON THE CLOSED CYCLE MHD SPECIALIST MEETING. WORKING GROUP OF THE JOINT ENEA: IAEA INTERNATIONAL MHD LIAISON GROUP AT EINDHOVEN, THE NETHERLANDS. September 20, 21 and 22, 1971.
TH-Report 72-E-29. April 1972. ISBN 90 6144 029 7

30. C.G.M. van Kessel and J.W.M.A. Houben.
LOSS MECHANISMS IN AN MHD-GENERATOR.
TH-Report 72-E-30. June 1972. ISBN 90 6144 030 0.

31. A. Veefkind.
CONDUCTING GUIDS TO STABILIZE MHD-GENERATOR PLASMAS AGAINST IONIZATION INSTABILITIES. TH-Report 72-E-31. October 1972. ISBN 90 6144 031 9.

32. J.E. Daalder and C.W.M. Vos.
DISTRIBUTION FUNCTIONS OF THE SPOT-DIAMETER FOR SINGLE- AND MULTI-CATHODE DISCHARGES IN VACUUM. TH-Report 73-E-32. January 1973. ISBN 90 6144 032 7.

33. J.E. Daalder.
JOULE HEATING AND DIAMETER OF THE CATHODE SPOT IN A VACUUM ARC.
TH-Report 73-E-33. January 1973. ISBN 90 6144 033 5.

34. Huber, C.
BEHAVIOUR OF THE SPINNING GYRO ROTOR.
TH-Report 73-E-34. February 1973. ISBN 90 6144 034 3.

35. Boeschoten, F.
THE VACUUM ARC AS A FACILITY FOR RELEVANT EXPERIMENTS IN FUSION RESEARCH.
TH-Report 73-E-35, February 1973, ISBN 90 6144 035 1.

36. Blom, J.A.
ANALYSIS OF PHYSIOLOGICAL SYSTEMS BY PARAMETER ESTIMATION TECHNIQUES.
73-E-36. 1973. ISBN 90 6144 036 X

37. Lier, M.C. van and R.H.J.M. Otten.
AUTOMATIC WIRING DESIGN.
TH-reprot 73-E-37. May 1973. ISBN 90 6144 037 8

38. Andriessen, F.J.
CALCULATION OF RADIATION LOSSES IN CYLINDRICAL SYMMETERICAL HIGH PRESSURE DISCHARGES BY MEANS OF A DIGITAL COMPUTER.
TH-report 73-E-38. October 1973. ISBN 90 6144 038 6

39. Dijk, J., C.T.W. van Diepenbeek, E.J. Maanders and L.F.G. Thurlings.
THE POLARIZATION LOSSES OF OFFSET ANTENNAS.
TH-report 73-E-39. June 1973. ISBN 90 6144 039 4.

40. Goes, W.P.
SEPARATION OF SIGNALS DUE TO ARTERIAL AND VENOUS BLOODFLOW, IN THE DOPPLER SYSTEM, THAT USES CONTINUOUS ULTRASOUND.
TH-report 73-E-40. September 1973. ISBN 90 6144 040 8

41. Damen, A.A.H.
A COMPARATIVE ANALYSIS OF SEVERAL MODELS OF THE VENTRICULAR DEPOLARISATION; *INTRODUCTION OF A STRING MODEL.*
TH-report 73-E-41. October 1973. ISBN 90 6144 041 6.

42. Dijk, G.H.M. van.
THEORY OF GYRO WITH ROTATING GIMBAL AND FLEXURAL PIVOTS.
TH-report 73-E-42. September 1972. ISBN 90 6144 042 4.